Two-dimensional turbulence analysis using high-speed visible imaging in TJ-II edge plasmas

1. Introduction

Transport in fusion devices is a phenomenon with a high degree of complexity. Localized layers where $\boldsymbol{E}\times\boldsymbol{B}$ shear stabilization mechanisms are likely playing a role have extensively been proved to have a beneficial impact in confinement. A reduction in turbulence amplitude is expected and measured [1]. However, few attempts have been made to study the effects of such a layer on the morphology of turbulent structures [2]. Two-dimensional (2D) images of edge plasma turbulence have been obtained by high-speed imaging in the visible range in the edge of tokamak devices [3], [4].

This article reports on a 2D visualization of transport in the plasma edge of the TJ-II stellarator by high-speed H_α imaging. A wavelet-based image analysis method is used to localize and characterize blob-like structures. The impact of shear flow and external biasing on turbulent structures is investigated by means of this method.

2. Experimental description

Experiments were carried out in TJ-II plasmas using electron cyclotron resonance heating (ECRH), with P_{ECRH} = 200–400 kW, B_T = 1 T, R = 1.5 m, $\langle a \rangle$ = 0.22 m, and ι(a) ≈ 1.6.

For the 2D turbulence studies presented here, two different cameras were used. The first model is a Princeton Scientific Instruments intensified camera with a CCD sensor (PSI-5), achieving recording rates up to 250,000 frames per second (fps). The storage capacity is 300 frames with 64 × 64 pixel resolution, thus giving 1.2 ms total recording time at maximum speed with an image every 4 ms. The second camera is a Phantom v7.1 by Photo-sonics International LTD, with CMOS sensor. Its recording speed is 120,000 fps with 64 × 64 pixel frame resolution. Recording durations can be of hundreds of milliseconds.

Neutral recycling at the poloidal limiter is used to light up the outer plasma region (ρ ~ 0.7– 1). The view plane is in a near-poloidal cross section with optimized B-field perpendicularity (see Fig. 1). The light cloud extent along field lines was measured and is in the range of a few centimeters (~10 cm). Projections of the field lines on the view plane can be seen in the upper left image of Fig. 4.

Bright structures are frequently seen with a spatial extent of a few centimeters. Those structures show predominant poloidal movements with typical speeds of 10^3–10^4 ms^{-1}, in agreement with the expected $\boldsymbol{E}\times\boldsymbol{B}$ drift rotation direction. Moreover, projection of the magnetic field lines on the image frame reveals little or no velocity component in the field line direction. With this light cloud thickness, long parallel structures can have a parallel velocity component not visible from the camera position.

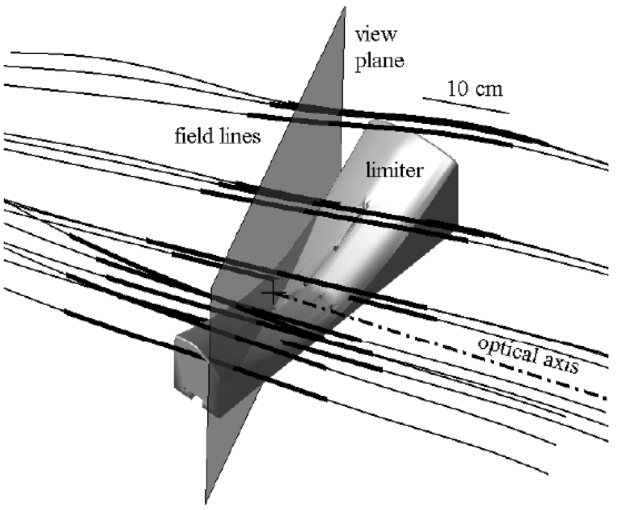

Fig. 1. View plane and field lines near the poloidal limiter used for plasma edge lighting. Broad lines stand for the toroidal extent of the light cloud.

3. Impact of edge shear layer on 2D turbulence structure

A naturally occurring shear layer has been observed in TJ-II edge plasmas [5, 6]. It is self-organized near marginal stability with fluctuations, the shearing rate being close to 10^5 s^{-1}. It is formed in certain magnetic configurations above a density threshold (~0.6×10^{19} m^{-3}), though its appearance is linked with several magnetic and plasma parameters [6]. The controllable occurrence of this shear layer allows us to study its impact on turbulent structures.

Several image sequences for shots with and without a shear layer were analyzed. Frame size in this series of shots was 11 cm × 11 cm, and the recording duration was 1.2 ms. During this small time window, line-averaged density is approximately constant.

The method described in Ref. [7] extracts the blobs on three different scales. These detected structures are then analyzed and labeled with a scale, an angle, and an aspect ratio. From the angular and aspect ratio histograms we extract the standard deviation (STD) of angular distribution and the percentage of elongated blobs,[1] respectively. This percentage is a measure of blob stretching, whereas the angular STD is an indication of the level of order of the

1. A blob is considered to be "elongated" when its aspect ratio is greater than 2.

blob population. Large STDs mean that blobs are randomly oriented; small ones mean that blobs point in roughly the same direction.

These blob statistical parameters are plotted against line-averaged electron density in Fig. 2 for the $k \sim 1.2$ cm^{-1} structures (statistics were significant only in this scale). In the top portion of Fig. 2 a clear reduction of angular dispersion is observed as density rises and a shear layer is developed. The bottom portion of Fig. 2. shows a slight though perceptible positive dependence of the percentage "% of elongated blobs" on the line-averaged density.

Mean H_α profiles were measured for these shots. For increasing densities, the images show higher H_α emission, but no reduction of the light cloud, which might be affecting our data interpretation, was observed.

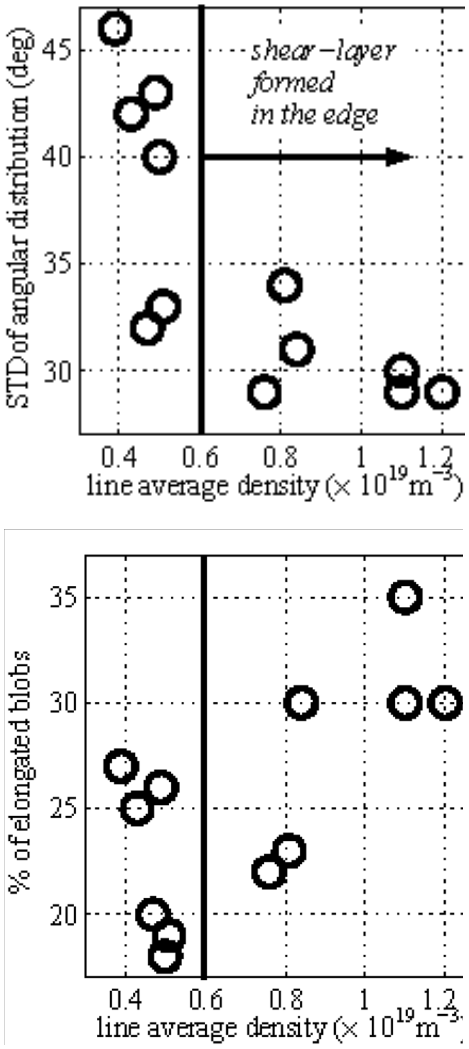

Fig. 2. Density dependence of the standard deviation of blobs angular distribution (top) and population of elongated blobs (bottom).

4. Turbulence structure modification during external biasing induced improved confinement regime

Improved confinement regimes are accessible in the TJ-II stellarator through external biasing [8]. The plasma edge is biased with a graphite electrode installed in a fast reciprocating probe drive. The electrode was inserted typically 2 cm inside the LCFS and biased with respect to one of the two TJ-II limiters [9].

The long recording capabilities of the Phantom v7.1 fast camera allowed us to study the effects of turning off the biasing from the improved to the normal regime. A 17-ms long shot with a 19 × 19 cm frame size was analyzed. First results confirm the deep impact of external biasing in plasma edge structures.

Figure 3(a) shows the evolution of the ratio of line-averaged electron density to H_α, evidencing the better confinement during biasing. In this time window, n_e is approximately constant (~ 0.6×10^{19} m^{-3}). The frame RMS (calculated as the square root of the sum to every pixel of the squared pixel intensity) reflects the relative increase in turbulence activity [Fig. 3(b)]. The number of turbulent structures detected at all three different scales also increases when biasing is turned off [Figs. 3(c)–3(e)] again reflecting an increase in turbulent activity. However, the increase is not the same for all the analyzed scales, being particularly intense for the intermediate scale ($k \sim 1.4$ cm^{-1}). It can be seen that the ratio of medium-scale ($k \sim 1.4$ cm^{-1}) to large-scale ($k \sim 0.7$ cm^{-1}) blob population changes from 0.4 during biasing to 0.8 after biasing. We emphasize that the number of blobs per frame in each scale is not to be taken as an absolute value, since smaller scales are more affected by noise and therefore the threshold for detection has to be more severe. However, this change in relative scale activity is a meaningful modification of turbulence structure.

The effect of biasing on turbulent structures was also noticeable in the standard deviation (STD) of the angular distribution [for the $k \sim 1.4$ cm^{-1} structures, it changes from 18º during biasing to 29º after it, see Fig. 2(a) for comparison], as well as in the percentage of elongated blobs [from 47% to 34% for $k \sim 1.4$ cm^{-1}; see Fig. 2(b)]. A similar tendency was found in the blobs with $k \sim 0.7$ cm^{-1}. Not enough $k \sim 2.8$ cm^{-1} structures were detected for significant statistics.

Figure 4 is an example of the structure detection applied to one frame during biasing (upper left image) and after biasing (lower left image). The continuous wavelet transform in three different scales extracts structures around wavelet scale: $k \sim 0.7$ cm^{-1} structures in the second column, $k \sim 1.4$ cm^{-1} in the third column, and $k \sim 2.8$ cm^{-1} in the fourth column. The relative increase can be seen in

medium-scale structures from the frame before biasing turn-off (top) to the frame after biasing (bottom).

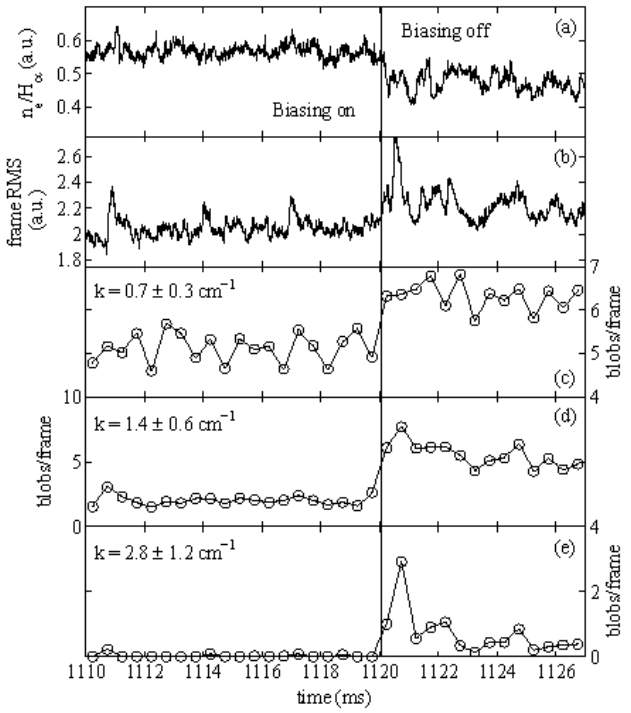

Fig. 3. Time evolution of (a) the ratio of electron density to H_α, (b) frame root mean square, and (c)–(e) 50-frame average number of structures per frame in different scales, during and after biasing (shot #13721).

5. Conclusions

Two-dimensional plasma edge turbulence was investigated by means of fast imaging in the visible range. A continuous wavelet-based method was used to localize and study the geometry of coherent turbulent structures (scale, aspect ratio and orientation angle) in different plasma regimes.

First, the impact of the naturally occurring shear layer, self-organized near marginal stability, on TJ-II edge turbulent structures was addressed. Experimental results show a reduction in the angular dispersion of $k \sim 1.2$ cm^{-1} blobs as the shear layer is established in the boundary, as well as a slight though sensible shift of the aspect ratio histogram toward higher values (Fig. 2). These results are consistent with the picture of the shear layer stressing blobs as well as ordering them. Neither significant changes in turbulence intensity (as the number of blobs detected) nor a clear reduction in turbulence scale could be detected with present fast camera experimental setup and analyzing method. It should be noted that spontaneous edge sheared flow and fluctuations are near marginal stability. However, probe measurements show that when sheared flow develops, the level of fluctuations decreases [6].

Second, the effect of external biasing on the blob relative populations of the three different scales analyzed ($k \sim 0.7$ cm^{-1}, 1.4 cm^{-1}, 2.8 cm^{-1}) was studied. An increase in all the analyzed scales was observed when biasing was removed. This increase is more noticeable for the intermediate scales, $k \sim 1.4$ cm^{-1}. During external biasing the standard deviation of these structures was significantly less than after biasing turn-off, and the aspect ratio histogram was relatively shifted toward higher values. This

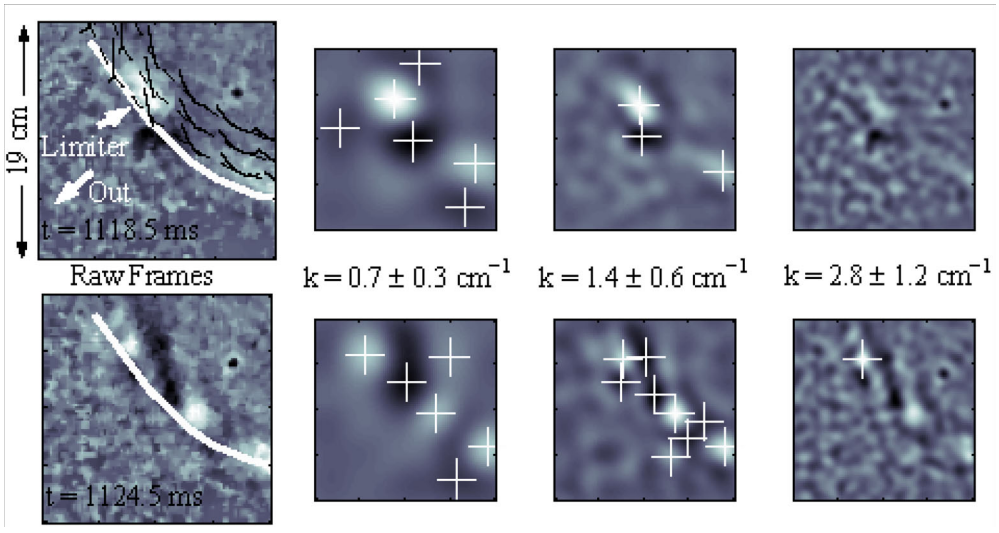

Fig. 4. Structure detection in two frames of shot 13721, during (top) and after biasing (bottom). White pluses indicate detected blob positions. In the upper raw frame: white solid line is the limiter ridge, black dashed lines are the intersections of magnetic surfaces ($\rho \sim 0.65, 0.75, 0.85$) with the view plane, and black solid lines are projections of the magnetic field lines inside the light cloud (30 cm long).

result shows a deep modification in the *k* power spectrum during external-biasing-induced improved confinement regimes, not only in its integrated power but also in its shape.

J. A. Alonso., S. J. Zweben,[1] J. L. de Pablos, E. de la Cal, C. Hidalgo, T. Klinger,[2] B.Ph. van Milligen, M. A. Pedrosa, C. Silva,[3] H. Thomsen[2]
Laboratorio Nacional de Fusion, Asociacion EURATOM-CIEMAT, 28040 Madrid, Spain
[1] Princeton Plasma Physics Laboratory, Princeton, NJ, USA
[2] Max-Planck-Institut fur Plasma Physik, EURATOM Ass., 17491 Greifswald, Germany
3 Associacao Euratom/IST, Centro de Fusao Nuclear, Instituto Superior Tecnico
E-mail: ja.alonso@ciemat.es

References

[1] P. W. Terry, Rev. Mod. Phys. **72**, 109 (2000).

[2] H. Thomsen et al, in Proc. 32nd EPS Conference on Control. Fusion and Plasma Physics (ECA, Tarragona, 2005), p. P5.027.

[3] S. J. Zweben et al., Nucl. Fusion **44**, 134 (2004).

[4] J. L. Terry et al., Phys. Plasmas **10**, 1739 (2003).

[5] C. Hidalgo, M. A. Pedrosa, L. García, and A. Ware, Phys. Rev. E **70,** 1 (2004).

[6] M. A. Pedrosa et al., Plasma Phys. Control. Fusion **47**, 777 (2005).

[7] J. A. Alonso et al., in Proc. 32nd EPS conference on Control. Fusion and Plasma Physics (ECA, Tarragona, 2005), p. P5.027.

[8] C. Hidalgo et al, Plasma Phys. Control. Fusion **46**, 287 (2004).

[9] C. Silva et al., in Proc. 32nd EPS conference on Control. Fusion and Plasma Physics (ECA, Tarragona, 2005), p. P2.037.